EVALUATION OF THE ACCURACY OF A LASER SCANNER-BASED ROLL MAPPING SYSTEM

R.S. Radovanovic*, W.F. Teskey*, N.N. Al-Hanbali**
*University of Calgary, Canada
Department of Geomatics Engineering
rsradova@ucalgary.ca
**Al-Balqual Applied University, Jordan
Surveying and Geomatics Engineering Department

Working Group V/2

KEY WORDS : Laser Scanning, Surface Mapping, Industrial Metrology

ABSTRACT

In industries where material must pass over one or more machine rolls, determining the shape and orientation of the rolls is an important element in quality control and failure prevention. This paper presents the results of research evaluating the accuracy a precise (sub-millimetre), non-contract method of roll mapping based on the use of a three-dimensional, autosynchronous laser scanner.

The system produced obtains image data of a machine roll using a three-dimensional, auto-synchronous laser scanner developed by the National Research Council of Canada. This device can scan over almost any surface at speeds of 18 kHz and produce three-dimensional coordinates of surface elements within a 45^{o} field of view. These elements are then input into a least-squares adjustment to determine a best-fitting cylinder. The elements are then further projected onto the cylinder and their deviations output as a digital elevation map.

Initial testing of the laser-scanner itself indicates that the scanner can measure 5 mm deformations in the depth direction to an accuracy of 0.3 mm on a 15m stand-off distance. This accuracy degrades linearly to the 0.9 mm level for moves of 40 mm. Relative accuracy in the vertical direction is decreased by a factor of approximately two, due to systematic errors in the laser scanner.

Further experiments conducted show that the entire system is capable of detecting surface distortions at the 0.1 mm level. However, the accuracy of the system in determining the radius, location and orientation of the roll is much less (cm-level for radius and position, 10"-level for orientation) due to the scanner's poorer absolute accuracy at ranges greater than 2 m and limited arc observed.

1 INTRODUCTION

Many industries use processes in which material must pass over one or more machine rolls. Two common examples are the paper making and printing industries. In these industries, the shape and roughness of the machine roll is a crucial factor in the processing of the paper. For example, if the dihedral angle of a guide roll is not correct, the paper may bunch up or roll off of the roll, thus halting production. Similarly, a warped roll can adversely affect the quality of the paper produced. The same principle applies to the alignment of the rolls, since paper can break if two rolls are not parallel within certain tolerances (Sprent and Hudson, 1996).

As machine speeds increase, the tolerances on the shape and orientation of rolls become ever more stringent. In addition, increased production outputs drive up the costs associated with the down-time required to survey a suspect role. This makes the development of fast, cost-effective methods to accurately determine roll shape and orientation very attractive to industry.

This paper presents the results of research aimed at the establishing the accuracy of a precise (sub-millimetre), non-contact method of roll mapping developed by Radovanovic et al, 1999. The system is based upon a 3D auto-synchronous laser scanner and is a new method that provides both the deviations *on the entire surface* of the roll *and* the orientation of the roll itself.

2 ROLL MAPPING WITH A LASER SCANNER SYSTEM

The roll-mapping system developed by Radovanovic et al, 1999 is based upon a 3-D autosyncronous laser scanner developed by the National Research Council of Canada. The laser scanner is capable of high data rates (up to 18 kHz) and is fairly insensitive to lighting conditions since it uses a steered infra-red laser to illuminate target elements. Details of the scanner operation are given by Blais et al, 1988.

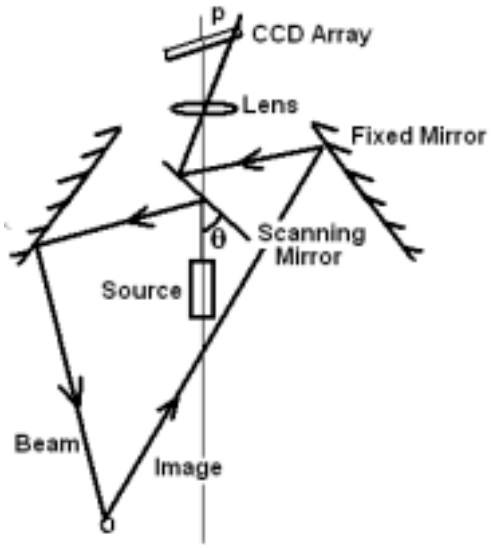

As shown in figure 1, a source laser beam is steered using a double-sided mirror into the scene. This beam intersects a target element, which is then imaged on the CCD array at a unique point p. given the value of p and the rotation of the mirror, θ, the x,z coordinates of the target element can be determined. The addition of a second rotating mirror to deflect the laser out of the page allows three dimensional scanning. The p,θ,ϕ to x,y,z transformation is quite complex and is thoroughly discussed in Al-Hanbali, 1998, as is calibration of the laser scanner.

In addition, the CCD array does not only record the position at which the laser spot is imaged, but also the intensity of the reflection. As a result, two images are produced, a depth image of the scene and an intensity image, analogous to a black and white photograph. A pair of images for a scene is shown in figure 2.

Figure 1. Principle of Scanner Operation

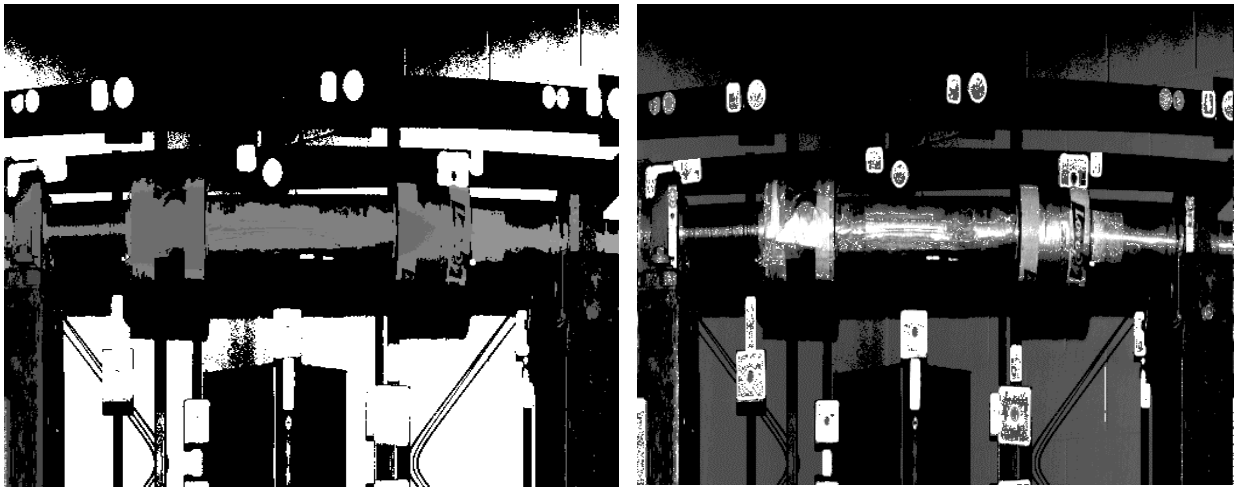

Figure 2. Laser Scanner Output. The left image is a depth image, while the right image is the corresponding intensity image.

2.1 Determination of Roll Parameters

The process of scanning a machine roll yields the x,y,z coordinates of visible surface elements in the laser scanner coordinate frame. Prior to using this data to generate a contour map of a roll surface, some datum surface must be defined. A contour map then describes the deviations of the actual roll surface from this theoretical reference. Fortunately, the coordinate data collected can be used to determine the best-fitting cylinder describing the roll via least-squares. A benefit of this scheme is that the orientation and radius of the roll so determined are useful parameters in the analysis of suspect machine rolls.

The mathematical formula describing a cylinder of radius R, centered at xo,yo and parallel to the z-axis (with respect to the laser scanner frame) is :

$$(x\text{-}xo)^2 + (y\text{-}yo)^2 = R^2 \qquad \text{(eq. 1)}$$

In the case of a cylinder that is not parallel to the z-axis and at an arbitrary position in space, the axis of the roll can be defined by two rotations (ϕ,ω) in the scanner frame. A third rotation is not necessary due to the rotational symmetry of a cylinder about its axis. This can be expressed by the product of two rotation matrices, namely :

$$\begin{bmatrix} x' \\ y' \\ z' \end{bmatrix} = R_y(\varphi) \cdot R_x(\omega) \begin{bmatrix} x \\ \cdot y \\ z \end{bmatrix} = \begin{vmatrix} \cos\varphi & \sin\omega\sin\varphi & -\sin\phi\cos\omega \\ 0 & \cos\omega & \sin\omega \\ \sin\varphi & -\sin\omega\cos\varphi & \cos\varphi\cos\omega \end{vmatrix} \cdot \begin{bmatrix} x \\ y \\ z \end{bmatrix} \qquad \text{(eq. 2)}$$

Substituting eq.2 into eq.1 then provides the mathematical description of an arbitrary cylinder, vis.:

$$(x\cos\varphi + y\sin\omega\sin\varphi - z\sin\varphi\cos\omega - xo')^2 + (y\cos\omega + z\sin\omega - yo')^2 - R^2 = 0 \qquad \text{(eq. 3)}$$

Thus a cylinder is completely defined by five parameters – radius, two rotations to define orientation, and two translations to define location. Given a set of n (x,y,z) coordinates on the surface of the cylinder, n equations of the form of eq. 3 can be written, and the parameters can be solved for via an implicit, non-linear least-squares adjustment. If several rolls are scanned at once, then the relative orientations of the rolls can be easily determined since ϕ,ω,xo, and yo all relate to the same scanner frame.

2.2 Projection Onto the Best-Fitting Cylinder and Creation of a Digital Elevation Map

Once the best-fitting cylinder parameters have been determined, individual elements can be projected onto the reference surface via the transformation :

$$\begin{bmatrix} x_p' \\ y_p' \\ z_p' \end{bmatrix} = R_y(\varphi) \cdot R_x(\omega) \cdot \begin{bmatrix} x_p \\ y_p \\ z_p \end{bmatrix} - \begin{bmatrix} xo' \\ yo' \\ 0 \end{bmatrix} \qquad \text{(eq. 4)}$$

This procedure simply rotates and translates points from the scanner frame into a reference frame centered on and aligned with the roll axis. The deviations of the points above and below the roll surface can then be calculated and given two dimensional planimetric coordinates via :

$$x_{mapping} = z_p' \qquad \text{(eq. 5)}$$

$$y_{mapping} = R \cdot \tan^{-1}\left(\frac{x_p'}{y_p'}\right) \qquad \text{(eq. 6)}$$

$$Height = \sqrt{(x_p'^2 + y_p'^2)} - R \qquad \text{(eq.7)}$$

where R is the solved radius of the roll.

Once all the scanned points have been projected into the mapping plane, they can be resampled into a regular grid using several different resampling techniques. Watson (1992) extensively reviews a wide variety of interpolation methods

including cubic convolution, linear interpolation and least-squares collocation. Currently, a simple quadratic-distance weighted interpolator is used since it is simple to implement, is computationally efficient, and preserves edge information better than a linear interpolation scheme.

Finally, the regularly gridded data is then used to create a digital elevation map of the surface of the machine roll. In the current system, elevations are simply quantized between 0 and 256 and output as a greyscale image. This allows quick assessment of general features on a suspect roll by a human analyst.

3 ACCURACY ASSESMENT OF THE ROLL MAPPING SYSTEM

One difficulty encountered while developing the roll mapping system described above was the sparse amount of data available regarding the performance and accuracy of the autosynchronous laser scanner used. Since the technology is relatively new, few studies have been completed on the accuracy of the scanner in metrology applications. As a result, evaluating the accuracy of both the scanner itself and the system as a whole were key priorities of the authors.

3.1 Laser Scanner Errors

Errors in the mapping system all have their source in the accuracy of the three-dimensional coordinates of sampled points. Errors in these points will both affect the determination of the roll parameters and directly result in elevation errors in the final mapping. For the application of roll mapping, the relative accuracy of points on the surface of the roll is much more important than their absolute accuracy (i.e. with respect to the scanner origin).

To estimate the relative accuracy of the laser scanner, the authors constructed a rigid plastic plate with etched circular targets. This plate was then mounted onto a precise translation stage and scanned at various translations to investigate if the scanner could detect the amount of induced deformation accurately. To insure the plate did not deform while moving, the stage was translated very slowly and smoothly.

An estimate of the accuracy in the z direction was determined by moving the stage away from the scanner, while an estimate in the y direction was calculated by moving the stage laterally. Note that the targets were well distributed in the scanner's field of view to randomize any systematic distortion in the scan.

This experiment was repeated for several ranges of movement and at stand-off distances of 1m, 5m, and 10m (near, mid and far field). The results are presented in figures 3 and 4.

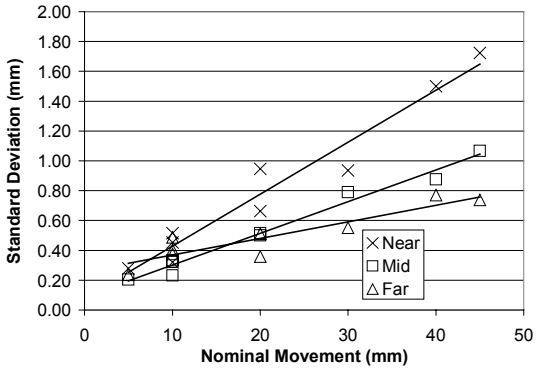

Figure 3. Accuracy of Deformation Detection in Y direction (lateral).

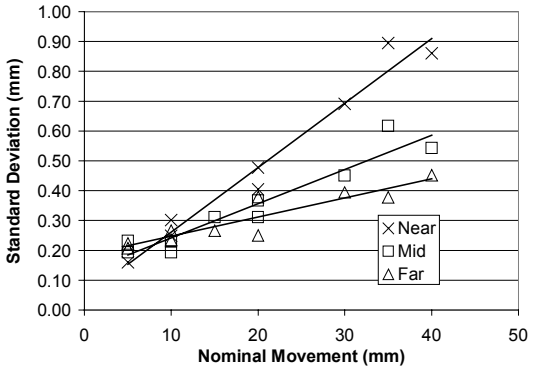

Figure 4. Accuracy of Deformation Detection in Z direction (depth).

Surprisingly, the standard deviations for both the y and z-direction movements are generally lower for points in the far-field. The reason for this is most likely due to uneven distortions in the laser scanner's field of view. As a result, points in the far-field do not move much in the laser scanner's field of view (see figure 5) and so are affected by the same distortions between epochs. These distortions then largely cancel out when the coordinates are differenced. This is not true for the points in the near position.

Similarly, when points move laterally in the scanner's field-of-view, they are affected by distortions of different magnitudes which do not cancel upon differencing. This explains why the relative accuracy of the scanner in the y direction (lateral) is poorer than the relative accuracy in the z direction (depth).

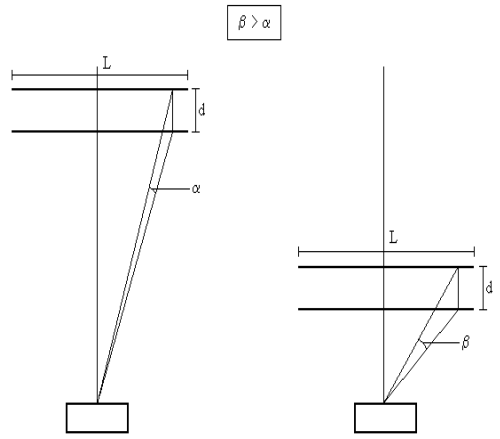

Figure 5. Effect of Movement at Different Depths

However, in the case of very small movements (less than 5mm) the near field has better accuracy. This is because at this level of movement, a point moves very little in the field of view regardless of standoff distance and other effects such as refraction make longer distance scans less accurate.

3.2 Mapping System Accuracy

The first test of the entire mapping system involved the scan of a vertical cylinder. The cylinder scanned is a 100mm (nominal) diameter rigid cardboard tube (sonotube). The surface of the roll is fairly smooth, but has sub-millimetre helical ridges running along the length of the tube as a result of the manufacturing process. The tube was placed approximately 100cm away from the scanner (in the optimal scan zone) and 61 629 points were imaged on the roll surface to be used in processing.

The results of the adjustment are shown in table 6.

Parameter	Adjusted Solution	Standard Deviation
Xo	1015.78 mm	0.05 mm
Yo	20.14 mm	0.01 mm
ω	176.6°	15.4 "
ϕ	0.1°	6.4 "
R	120.96 mm	0.05 mm

Table 6. Adjustment Results for Smooth Sonotube

Note that the standard deviations of the solved parameters are extremely small. The authors believe that this is an overly optimistic estimate of the accuracy of the solutions since the actual values of the solution can vary significantly depending on the subset of scanned points used in the adjustment. The extreme number of points used is the culprit for this optimistic indication of accuracy since neighboring points contribute very little information due to high correlation – a fact not contained in the diagonal covariance matrix used. Thus the redundancy of 61624 (61629 observations, five parameters) is misleading. To be rigorous, a covariance function should be calculated for the data and a weight matrix with off diagonal elements used in the adjustment.

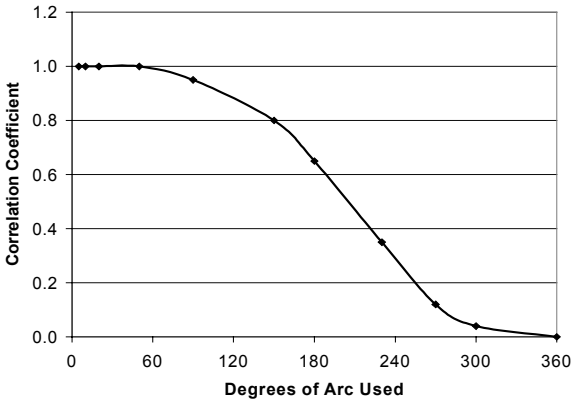

Figure 7. Correlation Between xo and R for Various Observed Degrees of Arc.

Also, note that the radius of 120 mm is significantly different than the nominal radius of 100mm as measured with a steel scale. This is due to the low degree of arc measured, which causes high correlation in the solutions for the radius and the standoff distance (xo) as shown in figure 7. A possible solution to this problem is to scan the roll from several different angles and joining successive images together to obtain a higher effective degree of arc observed. However, this would require mounting targets on the roll to act as tie-points in successive images.

Nonetheless, a digital elevation map for the roll was created using the parameters in Table 6. Figure 8 then shows the resulting digital elevation map for the roll. The diagonal lines are the effects of the sub-millimetre ridges on the surface of the sonotube.

Finally, note that variations in the surface heights are smooth and range in magnitude from +2 to –2 mm, which are reasonable considering the construction of the tube. Unfortunately, the above test cannot produce direct estimates of the accuracy of the roll mapping system since no other method was available to confirm that the distortions visible in figure 8 actually existed, and were not simply the result of errors in the laser scanner measurement, or subsequent processing.

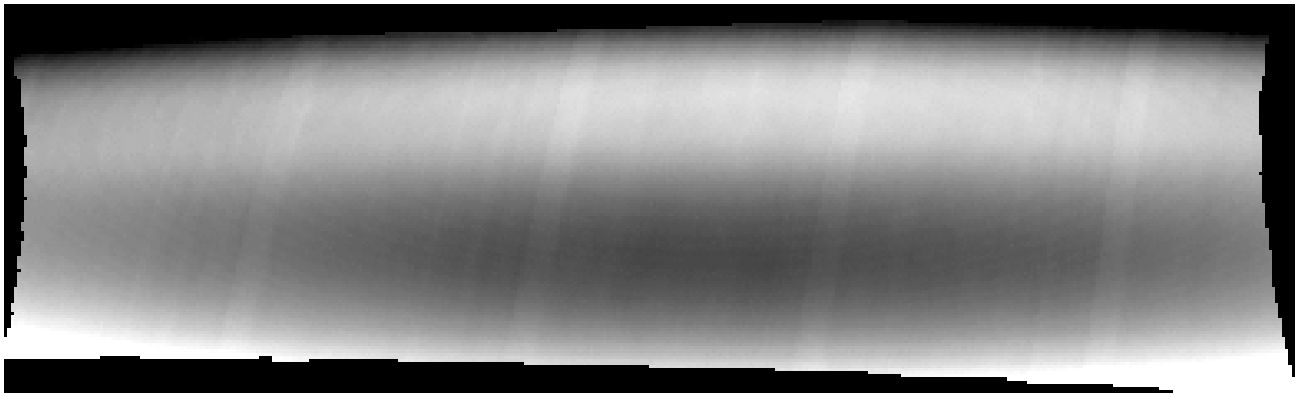

Figure 8. Elevation Map of a Smooth Sonotube. Lighter areas indicate points above the reference cylinder, while dark areas lie below the reference cylinder. Heights vary from 2.1 mm to –1.8 mm.

As a result, the authors performed another test using a roll with known surface distortions. Since it is very difficult to actually measure the distortions of a surface using any conventional method, the authors attached several pieces of wire of known diameter to a 12cm diameter plastic pipe, thus inducing known deformations onto the surface.

The same procedure was followed in this test as for that of the smooth sonotube. The corresponding elevation map of the roll is shown in figure 9. The presence of the wires are revealed quite readily as light ridges in the image. Note that the dark "holes" in the elevation map are areas where either specular reflection occurred off the wires, or spots that the scanning beam could not illuminate due to shadow effects.

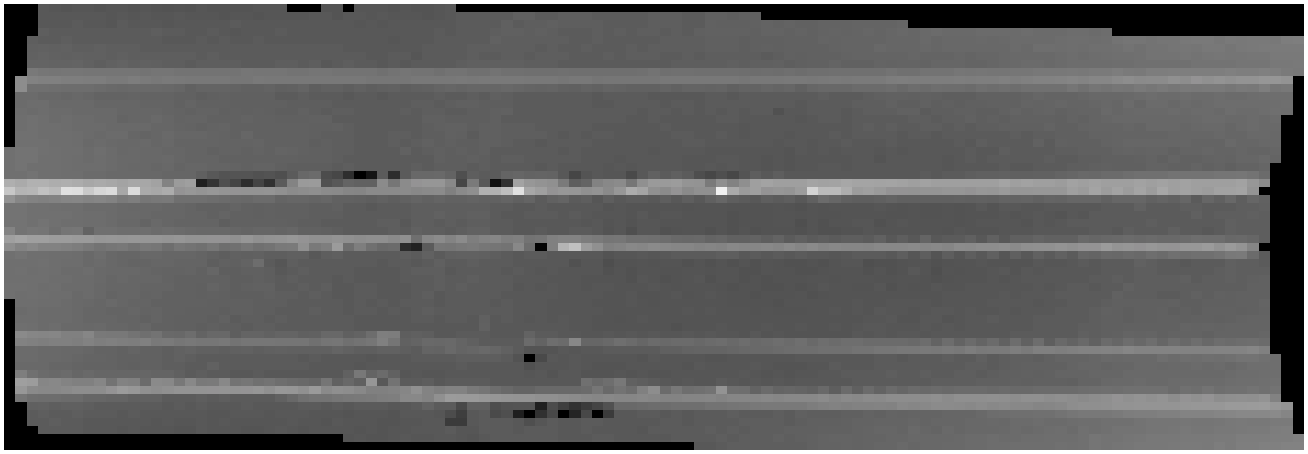

Figure 9. Elevation Map of Pipe with Controlled Distortions. Heights vary from –4.85 mm to 3.82 mm.

To quantitatively analyze the accuracy of the system in measuring distortions in the roll surface, five cross sections across the wire paths were taken and plotted in figure 10. Since the image is a greyscale, the height variations have been quantized into the range 10 to 256, but can be converted to linear units as described below. Surprisingly, the large wire proved to be the least consistent. This is due to noise from specular reflection and shadow effects as mentioned above.

Finally, the average wire diameter was calculated for each wire using the cross sectional data. Points for each cross section on either side of the peak were averaged to provide a "base" gray scale elevation. The peak value in each cross-section was then averaged to provide the "peak" greyscale elevation. These were then converted to linear units via

$$Diameter = (z_{peak} - z_{base}) \cdot \frac{H_{high} - H_{low}}{256 - 10} \qquad \text{(eq. 8)}$$

where H_{high}, H_{low} … highest and lowest elevations on the map

These are compared to the measured diameters in Table 11. The reference diameters were determined by measuring the wire diameter in three positions with a digital micrometer (least count 0.01 mm) and averaging the set.

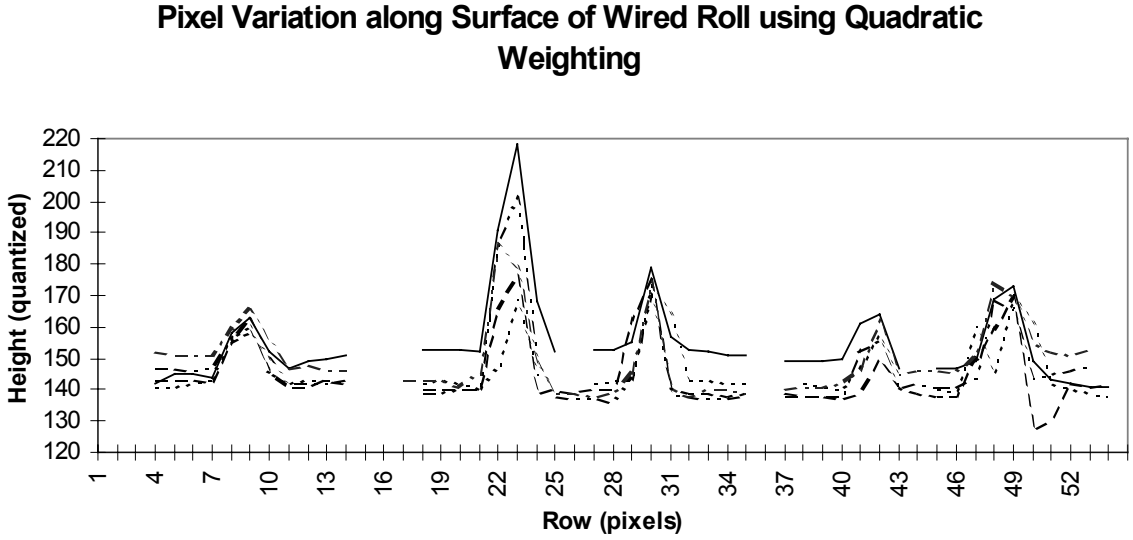

Figure 10. Cross-sections of Pixel Variations Along Wired Roll

Wire	Measured Diameter (mm)	Scanned Diameter (mm)	Error (mm)
1	1.000	0.961	0.039
2	2.420	2.431	-0.011
3	1.580	1.740	-0.160
4	1.000	0.999	0.001
5	1.530	1.482	0.048
		Mean	**-0.016**
		Standard Deviation	**0.084**

Table 11. Analysis of Scanner Wire Diameters

As can be seen, this mapping system is definitely capable of resolving small surface deviations extremely accurately. This is especially significant when one considers that the width of the structure measured is on the order of a few millimetres.

4 CONCLUSIONS

The roll mapping system described herein uses a laser scanner image of a roll to determine the parameters of the best-fitting cylinder given minimal user input. A greyscale elevation map of the visible surface of the roll is then automatically generated. Thus, the authors are confident that the basis of an operational roll mapping system has been established. This system is able to perform roll surveys in a fraction of the time required by conventional methods. In addition, the greyscale map is a feature previously unachievable by any method.

In particular, the system shows great promise in detecting small variations in a roll surface at the 0.1 mm level. The appearance of the ridges in the sonotube maps and the accuracy of the wire gauge determination are proof of this. Of course, further tests of the system's absolute accuracy are required, especially in determining the accuracy of the system for determining roll orientation and location. It may be possible to test this by surveying a roll using conventionally techniques and targets pasted to the roll. The results of the conventional survey can then be compared to those from the roll mapping system.

Nonetheless, the authors believe that the accuracy of the roll determination will remain the weak point in the system. Unfortunately, this is primarily due to the limited degree of arc observed. Future work will focus on effectively meshing several views of the roll in different rotational positions, probably using targets on the roll and the intensity file supplied.

Overall, the authors are satisfied that the objectives of this study were accomplished. A non-contact, fast method of static roll mapping was developed using a 3D auto-synchronous laser scanner. This system shows great promise in industrial applications provided a better understanding of the error characteristics of the scanner is gained.

ACKNOWLEDGEMENTS

The aid of James Thompson and Reid Egger in processing scanner images and in developing the roll mapping system is greatly appreciated. As well, the work completed was partially funded by grants from the National Sciences and Engineering Research Council of Canada.

REFERENCES

Al-Hanbali, N.N.,1998. Assessment of a Laser Scanning System for Deformation Monitoring Applications. Ph.D. Thesis. Department of Geomatics Engineering, The University of Calgary, Calgary, Canada.

Blais, F., M. Rioux, and J.A. Beraldin,1988. "Practical Consideration for a Design of a High Precision 3-D Laser Scanner System." Proceedings. SPIE, vol. 959, pp. 225-246.

Radovanovic, R.S., J. Thompson, R. Egger, and W.F. Teskey,1999. Use of a Laser Scanner System for Precise Roll Surface Mapping. Coordinate Measurement Systems Committee 1999. Seattle, July 26-30, 1999. 10 pp.

Sprent, A and A.J. Hudson,1996. "Paper Mill Alignment Surveys." Proceedings of the 8th International FIG Symposium in Deformation Measurements. Hong Kong, June 25-28, pp. 91-96.

Watson, D.F.,1992. Contouring: A Guide to the Analysis and Display of Spatial Data. Pergamon Press, Oxford.